

PACS numbers: 42.55.Lt; 42.65.Hw; 42.65.Re; 52.50.Jm
DOI: 10.1070/QE2009v039n07ABEH014090

Self-action of a high-power 10-μm laser radiation in gases: control of the pulse duration and generation of hot electrons

V.M. Gordienko, V.T. Platonenko, A.F. Sterzhantov

***Abstract*. The propagation of ultrashort 10-μm laser pulses of power exceeding the critical self-focusing power in xenon and air is numerically simulated. It is shown that the pulse duration in certain regimes in xenon can be decreased by 3 – 4 times simultaneously with the increase in the pulse power by 2 – 3 times. It is found that the average energy of electrons in a filament upon filamentation of 10-μm laser pulses in air can exceed 200 eV. The features of the third harmonic and terahertz radiation generation upon filamentation are discussed.**

Keywords: *filamentation, laser radiation self-action, pulse compression, hot electrons.*

1. Introduction

An investigation of phenomena taking place in superstrong optical fields is one of the rapidly developing fields in modern physics. Progress in this field is determined to a great extent by advances in the methods of generating near-IR femtosecond pulses which provided the observation of principally new phenomena in nonlinear optics and plasma physics and opened up new prospects in the technology of X-ray sources, the acceleration of charged particles, and other fields. Note that the development of high-power femtosecond laser systems in our country was initiated by S.A. Akhmanov at the Moscow State University [1].

Many studies with the use of intense laser radiation are devoted to analysis of the extreme states of matter, which can be obtained both in vacuum [2] and by the transport of laser radiation through gases [3, 4] or condensed media [5]. In addition, the propagation of ultrashort light packets of powers exceeding the critical self-focusing power in the atmosphere and other media are being actively investigated. One of the main phenomena observed in this case is the filamentation of radiation, which is used in spectroscopic lidars of a new generation and in the remote spectroscopy of solid objects [6]. The self-action of near-IR ultrashort light packets in gas media, in particular, in the atmosphere attracts great attention due to the possibility of radiation channeling over large distances, the transformation of the pulse spectrum and duration, and other phenomena related to the dependence of the refractive index on the radiation intensity [7].

It is reasonable that similar processes can proceed in the case of 10-μm ultrashort pulses generated by high-pressure CO_2 [8, 9] or N_2O [10] lasers. The power of such pulses is sufficient for obtaining the self-action regime and their duration is usually somewhat longer than a picosecond, but can also be subpicosecond [8].

Obviously, the character of self-action effects should depend considerably on the radiation wavelength λ. The self-focusing of light packets changes with increasing the radiation wavelength in the following way. Because the compression of a light beam during self-focusing in gases is mainly limited by the field ionisation, we can expect that the radiation intensity obtained in the filamentation regime weakly depends on the wavelength.

The critical self-focusing power is proportional to λ^2, and therefore the increase in the wavelength by an order of magnitude should result in the increase in the filament cross section by two orders of magnitude. The maximum power of a beam which can be channelled without the passage to multiple filamentation should also increase by two orders of magnitude [11]. For $\lambda = 1$ μm in air, this power is close to 5 GW [12], so that it will be ~ 0.5 TW in the 10-μm region. The electron oscillation energy in the light field is also proportional to λ^2. The average value of this energy ('pondermotive energy') is $\lambda^2 r_e I/2\pi c$ ($r_e = e^2/mc^2 = 2.82 \times 10^{-13}$ cm is the classical electron radius and I is the radiation intensity), so that the increase in λ by an order of magnitude will result in the increase in the pondermotive electron energy in a filament by two orders of magnitude. This should lead to a drastic increase in the efficiency of processes involving 'hot' electrons. Thus, the propagation of the high-power 10-μm radiation in gases (in particular, in the atmospheric air) is characterised by specific features requiring a detailed analysis.

In this paper, we studied numerically the self-action of picosecond 10-μm radiation packets in air and xenon and their applications.

2. Calculation model

We described a light wave in calculations by the equation [13]

V.M. Gordienko, V.T. Platonenko Department of Physics, M.V. Lomonosov Moscow State University, Vorob'evy gory, 119991 Moscow, Russia; e-mail: gord@phys.msu.ru;
A.F. Sterzhantov International Laser Center, M.V. Lomonosov Moscow State University, Vorob'evy gory, 119991 Moscow, Russia

Received 24 February 2009
Kvantovaya Elektronika **39** (7) 663 – 668 (2009)
Translated by M.N. Sapozhnikov

$$2ik\left(1+\frac{i}{ku}\frac{\partial}{\partial\tau}\right)\frac{\partial}{\partial z}A=\hat{D}A-i\omega\frac{4\pi}{c^2}\left(1+\frac{i}{\omega}\frac{\partial}{\partial\tau}\right)j_a. \quad (1)$$

Here, $A(r,z,\tau)$ is the amplitude of the electric field strength $E=A\exp[i(kz-\omega\tau)]+\text{c.c.}$;

$$\hat{D}A=\int\left[\left(k(\omega)+\frac{\Omega}{u}\right)^2-k^2(\omega+\Omega)-\nabla_\perp^2\right]$$

$$\times A_\Omega\exp(-i\Omega\tau)d\Omega;$$

$A_\Omega=(2\pi)^{-1}\int A(\tau)\exp(i\Omega\tau)d\tau$ is the Fourier transform of the amplitude; $k(\omega)=\omega n_0(\omega)/c$; n_0 is the linear refractive index; u is the group velocity of light; $\tau=t-z/u$; t is the time in the laboratory coordinate system; j_a is the amplitude of the nonlinear component of the current density $j_{nl}=j_a\exp[i(kz-\omega\tau)]+\text{c.c.}$ The amplitudes A and j_a are treated as scalar quantities, and the light beam is assumed axially symmetric. Equation (1) is solved by the method of splitting over physical parameters. By neglecting the first or second terms in its right-hand side, we obtain two equations. The first equation describes only dispersion and diffraction, while the second one describes only nonlinear processes. They are solved in each interval δz by turn (the solution of the first equation is transferred to the beginning of the interval and is used as the initial value in the solution of the second equation). The equation describing dispersion and diffraction has in the spectral representation the form

$$2ik\left(1+\frac{\Omega}{ku}\right)\frac{\partial}{\partial z}A_\Omega=-\nabla_\perp^2A_\Omega$$

$$+\left[\left(k+\frac{\Omega}{u}\right)^2-k^2(\omega+\Omega)\right]A_\Omega. \quad (2)$$

The solution of this equation (Schrödinger equation) and the passage from the time representation to the spectral one and vice versa are performed comparatively simply and do not require a special discussion. In the equation describing nonlinear processes, we neglect the difference of operators

$$\left(1+\frac{i}{ku}\frac{\partial}{\partial\tau}\right)\text{ and }\left(1+\frac{i}{\omega}\frac{\partial}{\partial\tau}\right),$$

because the group and phase velocities in conditions under study almost coincide. As a result, the equation takes the form

$$\frac{\partial}{\partial z}A=-\frac{2\pi}{c}j_a. \quad (3)$$

Nonlinear currents. The amplitude j_a of the current density is written as the sum $j_a=j_e+j_{n2}+j_f$. The term j_e (the free carrier current density) is calculated in the Drude model from the expression

$$j_e=i\frac{N_e e^2}{m(\omega+iv)}A, \quad (4)$$

where N_e is the free electron concentration and v is the elastic collision frequency. The latter depends, generally speaking, on the electron temperature, but this dependence is comparatively weak [14] and was neglected in calculations. It was assumed that $v=10^{13}\ \text{s}^{-1}$ in air and $5\times10^{12}\ \text{s}^{-1}$ in xenon at a pressure of 0.25 atm used in calculations (information on the elastic cross sections for collisions of electrons with atoms and molecules is presented in [14]). The term j_{n2} takes into account the Kerr nonlinearity of the refractive index and can be expressed in terms of the polarisation amplitude p_{n2}: $j_{n2}=-i\omega[1+(i/\omega)(\partial/\partial\tau)]p_{n2}$.

The operator $(i/\omega)(\partial/\partial\tau)$ in this expression is omitted hereafter because expressions for the amplitude p_{n2} used below are determined in the adiabatic approximation by neglecting the quantities of the order of $\omega^{-1}(\partial/\partial\tau)p_{n2}$ [expression (2) is written in the same approximation]. Note also that the Kerr nonlinearity of the refractive index in molecular gases contains the 'instant' and 'inertial' terms. But the characteristic inertia time of the Kerr nonlinearity in air is small (about 60 fs [15]), and therefore we will neglect this inertia. As a result, we obtain

$$j_{n2}=-i\frac{\omega}{2\pi}n_0n_2IA, \quad (5)$$

where I is the light intensity; n_2 is the coefficient determining the Kerr addition to the refractive index $\delta n=n_2I$. For such a definition of n_2, we have the critical self-focusing power $P_{cr}\approx\lambda^2/4\pi n_0n_2$ (see [7, 16]). The term j_f describes the absorption of light related to the field ionisation. It follows from phenomenological considerations (the law of conservation of energy) that

$$j_f=\frac{cn_0}{4\pi}\frac{W(U_{ion}+U_{osc})}{I}, \quad (6)$$

where U_{ion} is the ionisation potential; $U_{osc}=\lambda^2r_eI/2\pi c$ is the pondermotive potential; and W is the field ionisation rate (in $\text{cm}^{-3}\ \text{s}^{-1}$). Because the radiation frequency is small, ionisation has the tunnelling nature. Its probability $W(I)$ is calculated by expressions obtained in [17].

Evolution of plasma density. The electron concentration N_e also changes in collision processes. However, the rigorous description of these processes is too cumbersome. We will consider the role of these processes by using a rough average electron model and the rate equation for the electron concentration

$$N_e=W+(w_{av}-1/\tau_{dec})N_e, \quad (7)$$

where w_{av} is the rate of avalanche ionisation and τ_{dec}^{-1} is the total rate of processes reducing the electron concentration (recombination, attachment, etc.). Estimates show that this rate is very small (in particular, due to the large pondermotive electron energy), and we neglect it below. The avalanche ionisation rate in the general case is not small, and, strictly speaking, it should be calculated as the average by the expression $w_{av}=N_a\int V(\varepsilon)\sigma(\varepsilon)f(\varepsilon)d\varepsilon$, where N_a is the atomic or molecular concentration; V, σ, and f are the ionisation rate and cross section and the electron energy distribution function, respectively. The electron concentration used in calculations could achieve the values affecting considerably radiation only when the pondermotive energy greatly exceeded the ionisation potential of atoms or molecules. In this case, the product $V(\varepsilon)\sigma(\varepsilon)$ comparatively weakly depends on energy [14] (decreasing approximately as $\varepsilon^{-1/2}$ with increasing energy). Within the framework of this paper, we assumed that the product $V(\varepsilon)\sigma(\varepsilon)$ is constant. The variation of this quantity near its maximum value in air ($\sim1.7\times10^{-7}\ \text{cm}^3\ \text{s}^{-1}$ [14]) showed

that avalanche ionisation weakly affects the results discussed below. The rate w_{av} was set equal to 4×10^{12} s^{-1}. The elastic collision frequency in (4) is calculated by using similar expressions. It also depends on temperature, but this dependence is relatively weak [14] and was neglected in calculations. The cross section for collisions of electrons with xenon atoms is approximately twice that for collisions with oxygen and nitrogen molecules [14]. However, the processes in xenon were simulated at a lower pressure of the latter at which the role of collisions was insignificant (the value of n_2 was estimated from the expression $n_2 = P_{Xe} 8 \times 10^{-19}$ cm^2 W^{-1} [18], where P_{Xe} is the xenon pressure in atmospheres).

3. Noble gas in a cell

Experiments with gases in a cell differ from experiments in the atmosphere by a small path length and a great number of freely varied parameters (gas pressure and composition, etc.). One of the aims of such experiments is the development of methods for reducing pulse duration. For this purpose, we simulated the propagation of radiation wave packets in xenon by varying the gas pressure, the pulse power and duration, and input beam parameters. It was assumed that the gas pressure in a cell was 0.25 atm and the input parameters of the wave packet were such that a Gaussian transform-limited pulse with the FWHM $\tau_p = 1.2$ ps and $A(z=0) \propto \exp(-r^2/r_0^2)$ arrived to the point $z = 0$ in vacuum. The input window of the cell is located at the point $z_{in} = -5z_d$, where $z_d = \pi r_0^2/\lambda$ is the diffraction length. By varying the peak pulse power P_p (in the region $P_{cr} \leqslant P \leqslant 3P_{cr}$) and the diffraction length z_d, we observed two different self-action regimes allowing the reduction of the pulse duration.

The filamentation regime is observed at large diffraction lengths and high peak intensities and is characterised, in particular, by the formation of the shock waves of the envelope at the trailing edge of the pulse. This is explained as follows. Because the electron density at a fixed point in the axial region of the beam increases with time, the rear layers of a light packet propagate in a medium with the higher electron density and, hence, with the smaller group velocity than front layers. Under theses conditions, a shock wave can be formed at the trailing edge of the pulse [7]. Obviously, this wave is formed first of all in the axial region of the beam, where the electron density is maximal. A short pulse can be selected in such a regime by using an aperture. This regime is illustrated in Figs 1 and 2. As a rule, the pulse formed in the axial region (selected by an aperture) contains a long pedestal and its power is lower than the initial peak power P_p. The pulse duration can be considerably (almost by an order of magnitude) shorter than its initial duration, but its control is complicated because of the chaotic structure of a filament (Fig. 1). Unfortunately, this regime can be simulated only for limited lengths. In the case of large lengths, calculations produce beats with a period determined by the time step of the computational scheme. Under our calculation conditions, the trailing edge duration at such lengths was already close to half the optical period, so that the slowly varying amplitude method and various averagings assumed in the calculations of currents and other quantities in equations (1)–(7) lose their validity. To study this stage of the light packet evolution correctly, it is necessary to develop more perfect methods.

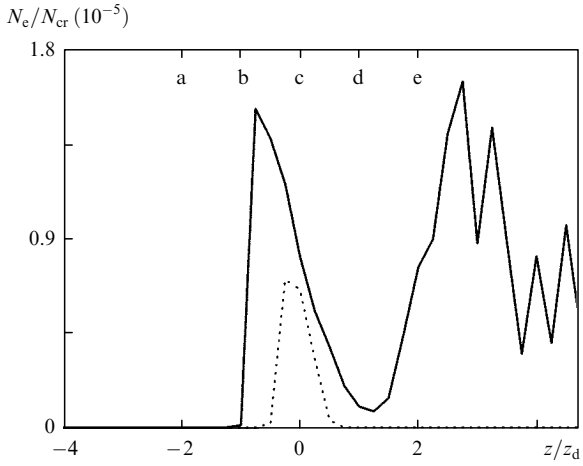

Figure 1. Normalised electron density on the laser beam axis as a function of the normalised coordinate z. The solid curve is the filamentation regime (calculated for the input power $P = 2.5P_{cr}$), the dotted curve is the single-focus regime ($P = 1.5P_{cr}$). The letters a, b, c, d, and e denote points with coordinates $Z_a = -2z_d$, $Z_b = -z_d$, $Z_c = 0$, $Z_d = z_d$, and $Z_e = 2z_d$.

The single focusing regime is observed for small diffraction lengths z_d and powers P_p only slightly exceeding the threshold power. The nature of single focusing at supercritical powers was discussed in [19] (see also [16]). In such a regime, the ionisation of matter sufficient to limit focusing

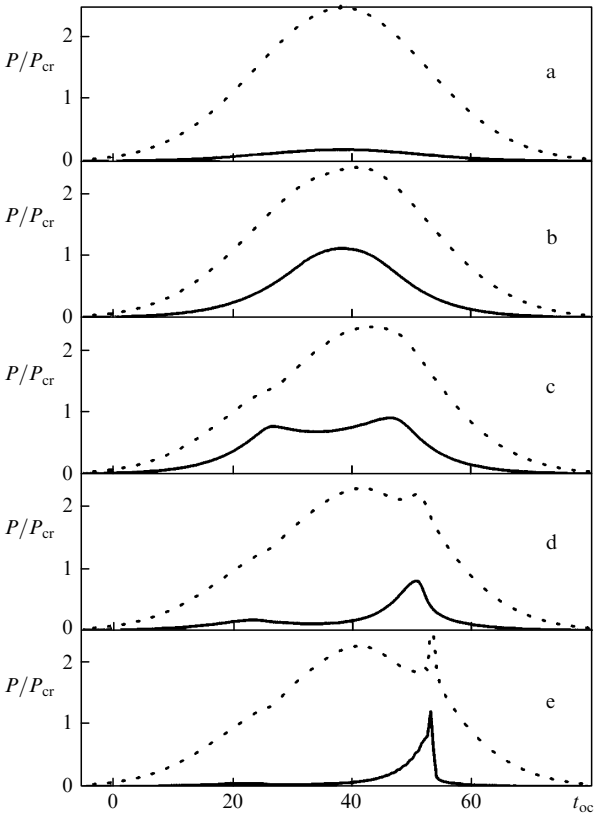

Figure 2. Light beam powers calculated in cross sections Z_a, Z_b, Z_c, Z_d, and Z_e. The dashed curve is the total beam power; the solid curve is the power propagating through an aperture of radius $0.12r_0$ (the aperture cross section is 0.03 of the initial beam cross section in the beam focus in the absence of self-action); t_{oc} is the time in light field periods.

occurs only over a small length, while the spatial structure of a beam and the dependence of the beam power on time behind the focus weakly differ from those realised in vacuum. The self-action is mainly reduced to the self-phase modulation. The central part of the pulse proves to be chirped in the positive direction and can be compressed in a medium with the anomalous group velocity dispersion (for example, in a NaCl plate [8, 10]. This regime is illustrated in Figs 1, 3, and 4. According to calculations, in this regime the pulse duration can be easily shortened by 3–4 times and its peak intensity can be increased by 2.5–3 times. As the initial power P_p is increased, these parameters increase, but up to a certain limit, which is caused by almost a jump-like passage to the filamentation regime. For the wave packet structure indicated above, the single-focus regime was realised in calculations for input powers not exceeding $2P_{cr}$. This range was expended at tighter focusing.

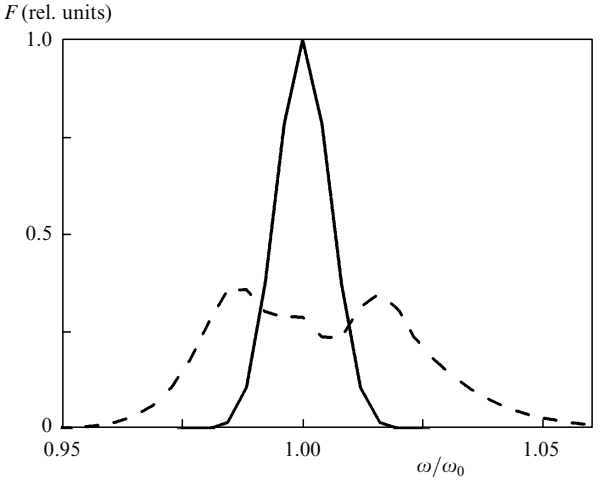

Figure 3. Spectra of a laser beam at the input (solid curve) and output (dashed curve) of a cell with xenon in the single-focus regime (the input power is $P = 1.5P_{cr}$). The frequency ω is normalised to the central frequency ω_0 of initial laser radiation.

The rough estimate of the width of the spectrum obtained in the single-focus regime at nearly critical powers can be performed analytically. In this case, the field amplitude can be written in the form $A \approx A_0 e^{i\varphi}$, where A_0 is the field amplitude in the absence of nonlinearity. Then, by neglecting ionisation, we obtain the relation $\partial\varphi/\partial z \approx kn_2 I$. By integrating this equation in infinite limits, we obtain the phase at the beam axis

$$\varphi(t) \approx \pi P(t)/P_{cr}. \quad (8)$$

By defining the instantaneous frequency as $\omega_{inst} = -\dot{\varphi}$ and assuming that the resulting width $\delta\omega$ of the spectrum is close to the difference between the maximum and minimum values of ω_{inst}, we obtain after simple algebraic transformations (for a Gaussian pulse)

$$\delta\omega \approx \sqrt{32\ln 2}\, e^{-1/2}(P_p/P_{cr})(\pi/\delta t),$$

which is approximately $3P_p/P_{cr}$ times larger than the width of a transform-limited pulse of duration δt. This estimate, as the time dependence of the phase (8), agrees with numerical calculations for $P_p \approx P_{cr}$. In the region $P > 1.5P_{cr}$, ionisation makes a noticeable contribution to the broadening of the spectrum, and the consideration presented above proves to be too rough. Formally, thus consideration is valid only for small phases (8). At the same time, this result is independent of the wavelength, and therefore the self-phase modulation in the single-focus regime can be probably used for reducing near-IR pulse durations (and increasing their power). Note that the pulse duration can be also reduced by using the two-stage compression scheme [20].

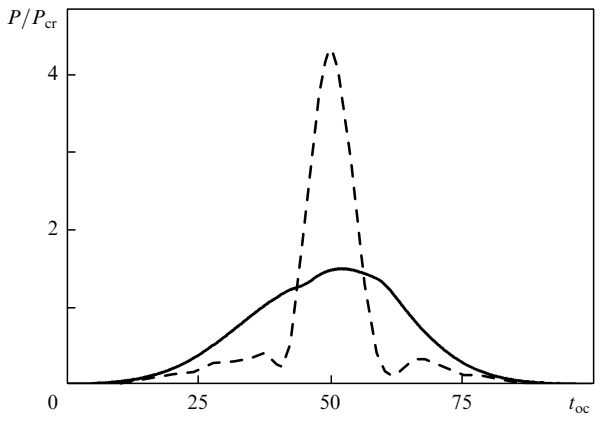

Figure 4. Light pulse subjected to self-action in front (solid curve) and behind (dashed curve) a 3.5-cm-thick NaCl plate.

4. Light packet in air

The propagation of a wave packet in air was simulated by assuming that $n_2 = 5.7 \times 10^{-19}$ cm^2 W^{-1} [18]. The power P_p was varied in the region $1.5P_{cr} \leqslant P_p \leqslant 2.5P_{cr}$, the diffraction length z_d was 40 m, the input parameters of the packet were specified at the point $z_{in} = -2z_d$ in the same way as in the case of a cell with xenon. The aim of the simulation was to elucidate whether it is possible to obtain the high radiation intensity (and thereby the high electron density and temperature) at a large distance from a radiation source. The properties obtained in calculations are qualitatively similar to those described above. For $P_p = 1.5P_{cr}$, a filament does not appear. For $P_p = 2.5P_{cr}$, a filament of length ~ 15 m with a peak electron density of $\sim 2.2 \times 10^{-5} N_{cr}$ ($N_{cr} = m\omega^2/4\pi e^2 \approx 10^{19}$ cm^{-3} is the critical power) is formed near the beam focus (i.e. at a distance of ~ 80 m). The evolution of radiation in the axial region in a fixed cross section is characterised by a pulse selected with a small-diameter aperture. The general properties of the behaviour of pulses observed in different cross sections in air weakly differ from those observed in xenon (Fig. 2). The parameters of these pulses change along the z axis not so regularly as for small z_d. The radiation intensity exceeding 10^{13} W cm^{-2} is maintained in a fixed region for no more than 300 fs. A small duration of this stage allows one to neglect avalanche ionisation [the term $w_{av}N_e$ in (7)] in analytic estimates.

To roughly estimate the maximum radiation intensity in a filament, we will use the following system of assumptions: the Kerr term in the refractive index and the term taking into account the contribution of free electrons compensate each other, i.e.

$$N_e/2N_{cr} = n_2 I, \quad (9)$$

The electron density can be estimated from the expression

$$N_e = W(I)\delta t/2, \quad (10)$$

and the ionisation probability averaged over the field period (see [21]) can be written in the simplified form

$$W(I) = \Omega \exp\left[-\frac{2}{3}\left(\frac{U}{U_H}\right)^{3/2}\frac{A_H}{A}\right], \quad (11)$$

where $U_H = 13.6$ eV; $A_H = e/r_B^2$ is the field strength produced by a proton at a distance equal to the Bohr radius; and $\Omega \approx 2\sqrt{A_H/A}\,U/\hbar$. By using these relations, we can obtain the expression for the radiation intensity

$$I = \frac{4}{9}\left(\frac{U}{U_H}\right)^3 I_H\left[\ln\left(\frac{U}{\hbar}\delta t\frac{N_a I_H^{1/4}}{N_{cr} n_2 I^{5/4}}\right)\right]^{-2}, \quad (12)$$

where $I_H = cA_H^2/8\pi \approx 3.5 \times 10^{16}$ W cm^{-2} and N_a is the density of ionised particles (in air, oxygen molecules). Because the argument of logarithm in this equation is very large ($\sim 10^{10}$), the equation can be easily solved by the method of successive approximations. For the same reason, even great errors in the estimate of this argument (for example, by one-two orders of magnitude) lead only to comparatively small (20 % – 40 %) errors in the estimates of I, which justifies the use of rough but simple expressions (9) – (11). According to equation (12), the maximum radiation intensity in a filament in air (for oxygen, $U = 12.2$ eV) is $\sim 2.2 \times 10^{13}$ W cm^{-2} and almost coincides with that obtained in calculations. For such intensity of the 10-μm radiation, the pondermotive electron energy exceeds 200 eV, while the oscillation energy amplitude exceeds 400 eV. It is known that the energy of the random (thermal) electron motion increases in each collision, on average, by the doubled pondermotive energy [14], so that an electron can acquire the energy ~ 1 keV already after two collisions. Clearly the presence of high-energy electrons should be accompanied by bremsstrahlung X-rays and excitation of molecules, in particular, to their deeply lying states. All this can lead to the development of new schemes for probing the atmosphere. Note that radiation intensity (12) weakly depends on the nonlinear refractive index n_2 and strongly depends on the ionisation potential.

5. Nonlinear transformations of high-intense 10-μm laser radiation in gases

In connection with the consideration performed above, we can also make the following comments concerning nonlinear transformations of high-intense 10-μm laser radiation in gases.

The propagation of ultrashort near-IR intense laser pulses ($I \sim 10^{13}$ W cm^{-2}) in gases is accompanied by the third harmonic generation (THG) [22]. The theoretical calculation of the THG process in the filamentation regime is a rather complicated problem. However, it is known from experiments with the 0.8-μm femtosecond laser radiation that the THG efficiency in the plasma formation [22] and filamentation [23] regimes achieves 0.1 %. Note that we studied earlier THG during the resonance interaction of 10-μm picosecond pulses with polyatomic molecules [24], however, we have failed to obtain so high THG efficiency. It should be expected that in the filamentation regime the 10-μm, 1-J pulses can be converted to the 3-μm range with energy more than 1 mJ. Such parameters become also practically important for the remote probing of the atmosphere.

It is known that filamentation of the near-IR femtosecond laser radiation in gas (air) is accompanied by conical terahertz emission [25]. The model of conical emission developed in [25] seems to be applicable in the case of filamentation of the 10-μm radiation. According to this model, conical emission is produced by wake oscillations excited by a laser pulse in a filament. The oscillation frequencies are determined by the electron concentration. According to calculations performed for the 10-μm range, these frequencies lie in the 10^{11}-Hz region. A rough analysis based on the results obtained in [25] shows that the energy emitted by wake waves is directly proportional to the product $E^2\lambda^2$, where E is the laser pulse energy. From this point of view, the passage to the longer-wavelength laser radiation seems advantageous. Note also that, by controlling the spectrum and focusing of laser radiation, it is possible to create a terahertz radiation source in a specified spatial region, in particular, in the region where an object being probed is located [25].

6. Conclusions

The propagation of ultrashort 10-μm laser pulses of power exceeding the critical self-focusing power in air and xenon has been simulated numerically. It has been shown that the pulse duration in xenon can be shortened by 3 – 4 times and their power simultaneously increased by 2 – 3 times in certain regimes. The method of shortening of ultrashort 10-μm laser pulses also allows the multistage (at least, two-stage) pulse conversion. In this case, the pulse shortening occurs with weak energy losses, i.e. the pulse peak power considerably increases.

Acknowledgements. This work was supported by the Russian Foundation for Basic Research (Grant Nos 08-02-01137a, 08-02-01245a, 08-02-90259-Uzb_a).

References

1. Akhmanov S.A., Gordienko V.M., Dzhidzhoev M.S., Krayushkin S.V., Kudinov I.A., Platonenko V.T., Popov V.K. *Kvantovaya Elektron.*, **13**, 1957 (1986) [*Sov. J. Quantum Electron.*, **16**, 1291 (1986)].
2. Mourou G., Tajima T., Bulanov S. *Rev. Mod. Phys.*, **78**, 309 (2006).
3. Li Y., Zhang J., Sheng Z., Teng H., et al. *Phys. Rev. Lett.*, **90** (16), 165002-1 (2003).
4. Gordienko V.M., Zhvania I.A., Makarov I.A. *Laser Phys.*, **18** (4), 380 (2008).
5. Juodkazis S., Nishimura K., Tanaka S., et al. *Phys. Rev. Lett.*, **96**, 166101-1 (2006).
6. Kasparian J., Wolf J.-P. *Opt. Express*, **16** (1), 466 (2008).
7. Akhmanov S.A., Vysloukh V.A., Chirkin A.S. *Optika femtosekundnykh lazernykh impul'sov* (Optics of Femtosecond Laser Pulses) (Moscow: Nauka, 1988).
8. Corkum P.B. *IEEE J. Quantum Electron.*, **21** (3), 216 (1985).
9. Biglov Z.A., Gordienko V.M., Platonenko V.T., Slobodnyuk V.A., Taranukhin V.D., Ten S.Yu. *Izv. Akad. Nauk SSSR, Ser. Fiz.*, **55**, 337 (1991).

10. Bravy B.G., Gordienko V.M., Platonenko V.T., Rykovanov S.G., Vasiliev G.K. *Proc. SPIE Int. Soc Opt. Eng.*, **6735**, 67350L (2007).
11. Kandidov V.P., Kosarev O.G., Koltun A.A. *Kvantovaya Elektron.*, **33**, 69 (2003) [*Quantum Electron.*, **33**, 69 (2003)].
12. Couairon A., Tzortzakis S., Berge L., et al. *J. Opt Soc. Am. B*, **19** (2), 118 (2002).
13. Mikhailova Yu.M., Platonenko V.T., Chjen C. *Zh. Eksp. Teor. Fiz.*, **135**, 211 (2009).
14. Raizer Yu.P. *Gas Discharge Physics* (Berlin: Springer-Verlag, 1991; Moscow: Nauka, 1987).
15. Oleinikov P.A., Platonenko V.T. *Laser Phys.*, **3**, 618 (1993).
16. Shen Y.R. *The Principles of Nonlinear Optics* (New York: John Wiley & Sons, 1984; Moscow: Nauka, 1989).
17. Perelomov A.M., Popov V.S., Terent'ev M.V. *Zh. Eksp. Teor. Fiz.*, **50**, 1393 (1966).
18. Nibbering E., Grillon G., Franco M., et al. *J. Opt. Soc. Am. B*, **14** (3), 650 (1997).
19. Wagner W.G., Haus H.A., Marburger J.H. *Phys. Rev.*, **175**, 256 (1968).
20. Couairon A., Biegert J., Hauri C., et al. *J. Modern Opt.*, **53** (1-2), 75 (2006).
21. Talebpour A., Yang J., Chin S. *Opt. Commun.,* **163**, 29 (1999).
22. Fedotov A.B., Koroteev N.I., Loy M., et al. *Opt. Commun.*, **133**, 587 (1997).
23. Akozbek N., Iwasaki A., Becker A., et al. *Appl. Phys. Lett.*, **89** (14), 143901-1 (2002).
24. Biglov Z.A., Gordienko V.M., Danilov E.O., Platonenko V.T., Slobodyanyuk V.A. *Proc. SPIE Int. Soc Opt. Eng.*, **2041**, 193 (1993).
25. D'Amico C., Houard A., Franco M., et al. *Phys. Rev. Lett.*, **98**, 235002 (2007).